High-heat-load monochromator options for the RIXS beamline at the APS with the MBA lattice

Cite as: AIP Conference Proceedings **1741**, 040046 (2016); https://doi.org/10.1063/1.4952918
Published Online: 27 July 2016

Zunping Liu, Thomas Gog, Stanislav A. Stoupin, Mary H. Upton, Yang Ding, Jung-Ho Kim, Diego M. Casa, Ayman H. Said, Jason A. Carter, and Gary Navrotski

High-Heat-Load Monochromator Options for the RIXS Beamline at the APS with the MBA Lattice

Zunping Liu[a], Thomas Gog[b], Stanislav A. Stoupin, Mary H. Upton, Yang Ding, Jung-Ho Kim, Diego M. Casa, Ayman H. Said, Jason A. Carter, and Gary Navrotski

Advanced Photon Source, Argonne National Laboratory, 9700 S. Cass Ave, Lemont, IL 60439, USA

[a)]Corresponding author: zpliu@anl.gov
[b)]gog@aps.anl.gov

Abstract. With the MBA lattice for APS-Upgrade, tuning curves of 2.6 cm period undulators meet the source requirements for the RIXS beamline. The high-heat-load monochromator (HHLM) is the first optical white beam component. There are four options for the HHLM such as diamond monochromators with refrigerant of either water or liquid nitrogen (LN2), and silicon monochromators of either direct or indirect cooling system. Their performances are evaluated at energy 11.215 keV (Ir L-III edge). The cryo-cooled diamond monochromator has similar performance as the water-cooled diamond monochromator because GaIn of the Cu-GaIn-diamond interface becomes solid. The cryo-cooled silicon monochromators perform better, not only in terms of surface slope error due to thermal deformation, but also in terms of thermal capacity.

INTRODUCTION

The source requirements for the resonant inelastic x-ray scattering (RIXS) beamline are determined by the need to access the energy at and near relevant transition metal absorption edges for a material under study. The overall energy ranges from 4.96 keV (Ti-K absorption edge) to 23 keV (Ru-K) [1]. The high-heat-load monochromator (HHLM) is the first optical white beam component. The cooling system of the diamond monochromator implemented at present has options for water and cryogenic refrigerants. The HHLM takes the immense power load from undulators and also serves as virtual source for downstream optics if the HHLM has large thermal deformation. A cryogenic-cooled diamond would be expected to have a higher power capacity. The available diamond crystal size and crystal quality are the limiting factors for a diamond HHLM. Silicon crystals are the best crystals in terms of crystal size and crystal lattice perfection.

The silicon HHLMs of either direct or indirect cooling have been successfully implemented at the 3rd generation of synchrotron facilities [2-4]. With the APS-Upgrade to the 4th generation storage ring source the source power density is expected to increase under MBA lattice operating at 6 GeV and 200 mA ring current. This study aims at evaluating which type of monochromator can best accommodate the (increased) power and power density for a modern spectroscopy beamline, where incident photon flux needs to be maximized.

EVALUATION

Finite element analysis (FEA) is applied for evaluation. The beam size at present operation in the RIXS beamline is controlled by a pair of white beam slits in order to maximize the photon flux after the HHLM, while the temperature reading of the thermal couple on the copper (Fig.1a) serves as a guidance. The white beam slits are at 27.63 m from source, while the diamond monochromators are at 2 m downstream. For comparison purpose all monochromators in Fig.1 are virtually put at the same location. The reflection plane is either C(111) or Si(111).

Proceedings of the 12th International Conference on Synchrotron Radiation Instrumentation – SRI2015
AIP Conf. Proc. 1741, 040046-1–040046-5; doi: 10.1063/1.4952918
Published by AIP Publishing. 978-0-7354-1398-6/$30.00

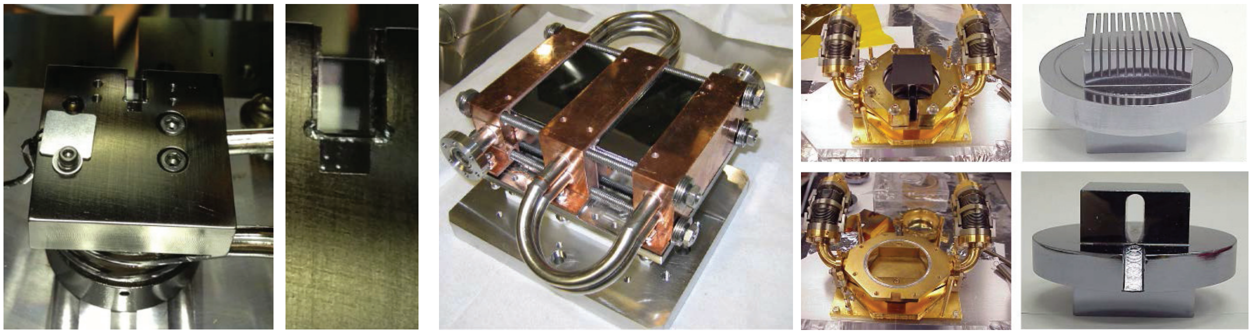

(a) (b) (c)

FIGURE 1. Monochromators: (a) Diamond; (b) Silicon, indirect cooling; (c) Silicon, direct cooling. The diamond mono is operating at the RIXS beamline, the indirect cooling silicon mono at Beamline 20-ID at the APS, while the direct cooling silicon mono at Beamline 19-ID (SBC-CAT) at the APS. OFHC copper is the support frame in (a) and (b).

The APS undulators U3.0 cm is the source at present operation at 7 GeV and 100 mA ring current, while the APS undulators U2.6 cm is chosen for evaluation under MBA lattice operating at 6 GeV and 200 mA current. The undulators tuning curve in Fig.2 shows the match in terms of energy ranges for these two scenarios. These tuning curves are generated through XOP software [5].

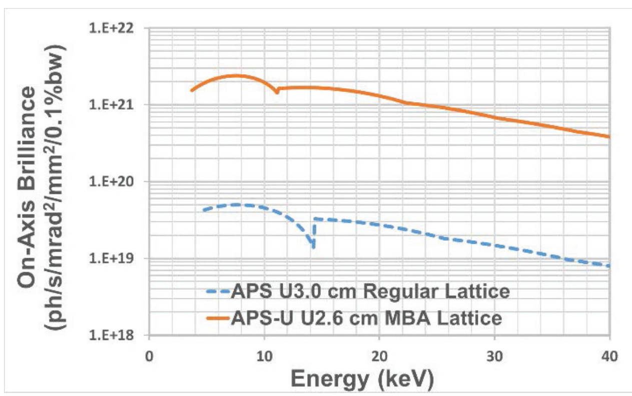

FIGURE 2. Undulator tuning curves

FEA Evaluation

The FEA procedure for silicon monochromators is well established, with details for the direct cooling one [3] and for the indirect cooling one [6]. For diamond monochromators the FEA procedure is the same, except that a diamond crystal is very thin. In present operation the RIXS beamline has a diamond-IIa crystal of 0.293 mm thick, 9.15 mm long and 4.2 mm wide. The same crystal is analyzed with water cooling and LN2 cooling scenarios.

As a benchmark the case of energy 11.215 keV (Ir L-III edge) is evaluated with the practical slits aperture (1.6 mm H x 0.6 mm V) at the present operation at the APS regular lattice. Figure 3(a) is the measured bandwith, which gives a peak-peak slope error 35 μrad. The FEA behavior of the water cooling diamond monochromator is shown in Fig.3b. For this case the peak-peak slope error is about 33 μrad with the absorbed power 12 W and peak power density 2.3 W/mm^2. By applying Bragg angle θ_B at this energy and the slope error $\Delta\theta$ at the surface to the following equation [7],

$$\Delta E = \Delta\theta E_i cot\theta_B \quad (1)$$

the resultant energy spread is about 1.5 eV. As a comparison the power absorption under the APS MBA lattice is also applied to the water cooling monochromator at the same energy. From the APS regular lattice to the MBA lattice the absorbed power increase to 15 W and the peak power density 2.8 W/mm^2. The resultant slope error increases to 40 μrad and the energy spread about 2 eV. Figure 3(a) suggests that power density, not total power, is the important parameter for the increase of the slope error and the energy spread.

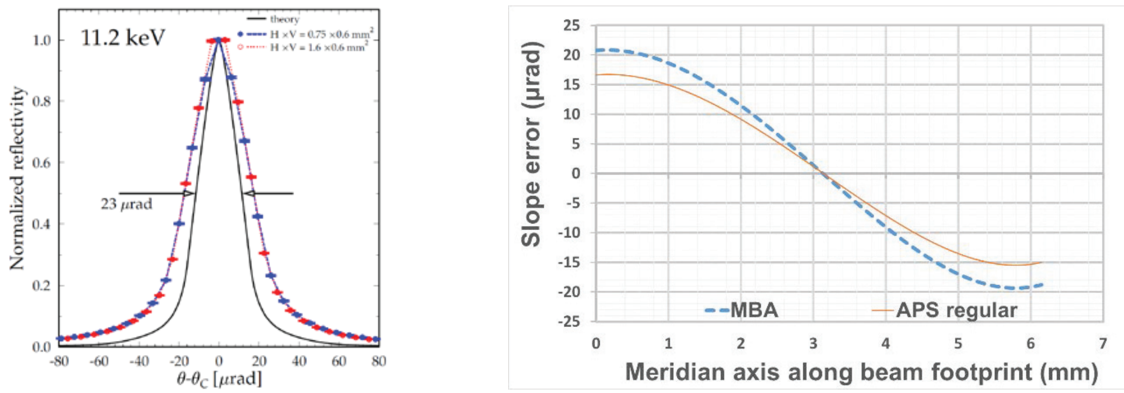

(a) (b)

FIGURE 3. Water-cooled diamond surface slope error due to thermal deformation at 11.215 keV. (a) Bandwidth. (b) Slope error.

Comparison of Monochromator Behavior

Figure 4 compares behavior of the diamond monochromators with water and LN2 cooling at the APS MBA lattice. The slits aperture is1.6 mm H x 0.6 mm V. The surface deformation is one order of magnitude smaller with LN2 cooling than water cooling. But the slope error of the diamond are in the same order for both water and LN2 cooling. The corresponding temperature profiles are shown in Fig.4(c). At room temperature the liquid GaIn of the Cu-GaIn-diamond interface allows diamond not deformed due to copper deformation. At cryogenic temperature GaIn is solidified so that the diamond is deformed with copper due to the solid bondage. As shown in Table 1 diamond has huge figure of merit at cryogenic temperature, which is neutralized by the copper due to the solid interface.

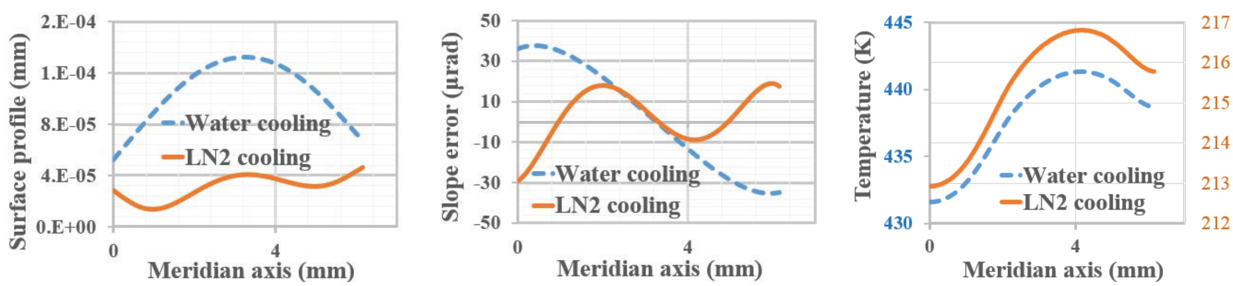

(a) (b) (c)

FIGURE 4. Diamond-IIa crystal behavior at 11.215 keV (Ir L-III edge) at the APS MBA lattice. (a) Surface profile, (b) Surface slope error, (c) Temperature profile.

TABLE 1. Figure of Merit

	Diamond		Silicon		OFHC Copper	
	80 K	300 K	80 K	300 K	80 K	300 K
K(W/m/K)	11700	2000	1000	150	558	401
α (1/K)	3.28×10^{-8}	1×10^{-6}	-5×10^{-7}	2.5×10^{-6}	8.3×10^{-6}	16.5×10^{-6}
$K/\alpha \times 10^6$	356700	2000	2000	60	67	24

Figure 5 compares behavior of the silicon monochromators with direct or indirect cooling. The slits aperture is1.6 mm H x 0.6 mm V. The current APS regular lattice and MBA lattice are both applied. For the specific design of both silicon monochromators in Fig.1, the indirect cooling has larger deformation (Fig.5a), smaller peak-peak slope error (Fig.5b) and lower peak temperature (Fig.5c). While switching from the APS regular lattice to MBA lattice, the deformation and temperature change are very small.

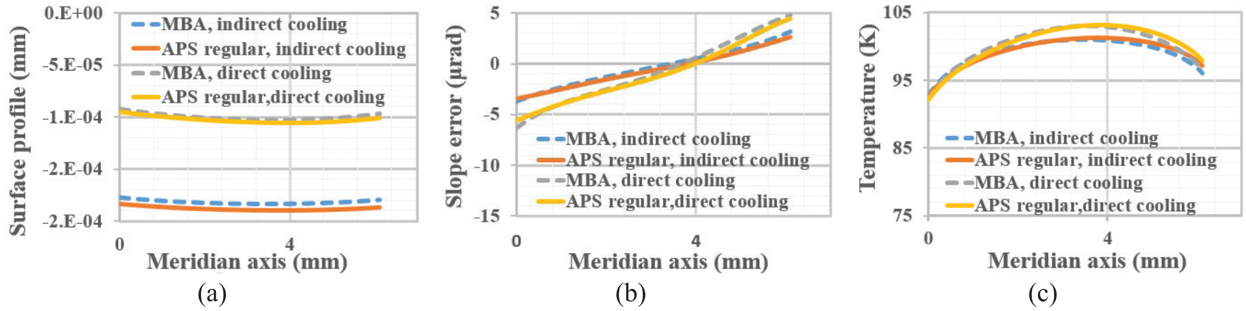

FIGURE 5. Silicon crystal behavior at 11.215 keV (Ir L-III edge) at the APS regular and MBA lattices. (a) Surface profile, (b) Surface slope error, (c) Temperature profile.

Figure 5 indicates that the indirect-cooling silicon monochromator has better performance than the other. When the absorbed power is simply scaled up with the same footprint, the peak-peak slope error changes with the power. As shown in Fig.6, the slope error increases with power up to about 180 W, then decreases with power up to 250 W, and increases dramatically when the power increases further. Because silicon has zero expansion coefficient at about 125 K and then expands at higher temperature, its surface will have a thermal bump when the peak temperature increases from 125 K. The thermal bump grows when temperature increases. The slope-power curve in Fig.6 indicates its work power capacity is 250 W.

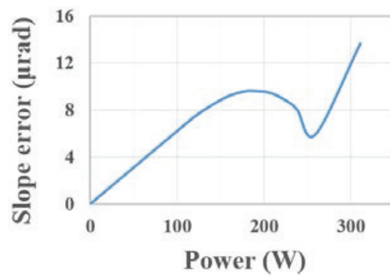

FIGURE 6. Surface slope error changes with absorbed power for the indirect cooling silicon monochromator.

SUMMARY

The APS undulator U2.6 cm provides desired energy range for the RIXS beamline at the APS-Upgrade. With the aperture size at present operation at 11.215 keV, the energy spread is negligible. The figure of merit of diamond at cryogenic-temperature is much higher than that of silicon. But its deformation at LN2 cooling is at the same order as water cooling. When GaIn of the Cu-GaIn-diamond interface becomes solid, the contact becomes bonded. For the specific design, the indirect-cooling silicon monochromator has smaller slope error than the direct-cooling one. The slope-power curve for indirect-cooling mono indicates its work power capacity is 250 W.

ACKNOWLEDGEMENTS

Mati Meron is acknowledged for his software for x-ray absorption calculation. Use of the Advanced Photon Source was supported by the U. S. Department of Energy, Office of Science, Office of Basic Energy Sciences, under Contract No. DE-AC02- 06CH11357.

REFERENCES

1. T. Gog, D.M. Casa, M.H. Upton, B. Brajuskovic and J. Carter, *RIXS Beamline FDR* (2014).

2. D.H. Bilderback, A.K. Freund, G.S. Knapp and D.M. Mills, *J. Synchrotron Rad.* 7, 53 (2000)
3. Z. Liu, G. Rosenbaum and G. Navrotski, *JPCS.* 493, 012009 (2014).
4. S. Stoupin, Z. Liu, S. Heald and D. Brewe, *SRI2015*
5. http://www.esrf.eu/Instrumentation/software/data-analysis/xop2.4
6. L.Zhang, M.Sanchez del Rio, G. Monaco, C.Detlefs, T.Roth, A.I.Chumakov and P.Glatzel, *J. Synchrotron Rad*. 20, 567 (2013)
7. T. Gog, D.M. Casa, A.H. Said, M.H. Upton, J.Kim, I.Kuzmenko, X. Huang, and R. Khachatryan, *J. Synchrotron Rad*. 20, 74 (2013)